

Probing the dynamics and coherence of a semiconductor hole spin via acoustic phonon-assisted excitation

N. Coste,¹ M. Gundin,¹ D. Fioretto,¹ S. E. Thomas,¹ C. Millet,¹ E. Medhi,¹ M. Gundin,¹ N. Somaschi,² M. Morassi,¹ M. Pont,¹ A. Lemaître,¹ N. Belabas,¹ O. Krebs,¹ L. Lanco,^{1,3} and P. Senellart¹

¹*Université Paris-Saclay, CNRS, Centre de Nanosciences et de Nanotechnologies, 91120, Palaiseau, France*

²*Quandela SAS, 10 Boulevard Thomas Gobert, 91120, Palaiseau, France*

³*Université Paris Cité, Centre for Nanoscience and Nanotechnology (C2N), F-91120 Palaiseau, France*

Spins in semiconductor quantum dots are promising local quantum memories to generate polarization-encoded photonic cluster states, as proposed in the pioneering Rudolph-Lindner scheme [1]. However, harnessing the polarization degree of freedom of the optical transitions is hindered by resonant excitation schemes that are widely used to obtain high photon indistinguishability. Here we show that acoustic phonon-assisted excitation, a scheme that preserves high indistinguishability, also allows to fully exploit the polarization selective optical transitions to initialise and measure single spin states. We access the coherence of hole spin systems in a low transverse magnetic field and directly monitor the spin Larmor precession both during the radiative emission process of an excited state or in the quantum dot ground state. We report a spin state detection fidelity of $94.7 \pm 0.2\%$ granted by the optical selection rules and a 20 ± 5 ns hole spin coherence time, demonstrating the potential of this scheme and system to generate linear cluster states with a dozen of photons.

The spins of carriers in solid-state systems are of great interest for optical quantum technologies [2], be it for distant quantum node entanglement [3, 4], envisioned photon-photon gates [5] or multi-photon entanglement [1, 6]. In 2009, Lindner and Rudolph (LR) [1] proposed a scheme which harnesses the spin properties of semiconductor quantum dots (QDs) to tackle the great challenge of deterministic photon cluster state generation. These multi-entangled photon states are highly sought-after to implement all-optical quantum networks [7, 8] as well as measurement-based quantum computing [9]. The LR scheme considers a periodically excited quantum dot electron spin precessing around a weak magnetic field: by synchronizing the excitation pulses and the spin precession period, a string of polarization-encoded single photons can be generated, forming a one-dimensional cluster state. The scheme is conceptually simple, robust and relies on polarization selection rules and a spin coherence time much longer than the radiative lifetime of the optical transitions. In order to obtain high multi-photon generation rate, a high photon collection efficiency is required which can be obtained by inserting the QD in cavities [10, 11]. Furthermore, if the photons are highly indistinguishable then higher-dimensional cluster states can be generated via fusion gates [12], which are instrumental for error-corrected quantum computing

A first implementation of the LR scheme was demonstrated using a spin system consisting of a dark QD exciton [6]. However, the use of non-resonant excitation limited the photon indistinguishability to $\approx 17\%$ [13]. More recently, a similar demonstration was demonstrated using a QD hole spin with a non-resonant scheme exploiting the fast emission of longitudinal optical phonons [13]. The use of optical-phonon relaxation allows for single-photon indistinguishabilities of over 90% for QDs in bulk, which typically have a nanosecond radiative lifetime. However,

the intrinsic time jitter of the LO phonon relaxation becomes comparable to the optical transition lifetime when the QD is inserted in a cavity and the photons indistinguishability is reduced [14].

The generation of highly indistinguishable photons has been reproducibly demonstrated through resonant excitation of QDs [15, 16], and with unparalleled efficiency when making use of microcavities [10, 11, 17]. However, resonant excitation schemes in a confocal microscopy require rejection of the resonant excitation laser through polarization filtering, which precludes polarization encoding of single photons and hence using the LR scheme. Alternative schemes have been proposed to address this difficulty, replacing the polarization degree of freedom by time bin encoding [18–20]. This is however more resource demanding as it involves an intense magnetic field and phase stabilization of the emitted photons. Longitudinal acoustic (LA)-phonon assisted excitation schemes have been proposed for the generation of single photons with near-unity indistinguishability as well as high occupation probability of the QD excited states [21–23]. In this scheme, phonon-assisted processes do not lead to time jitter of the photon emission since the phonon relaxation only takes place while the excitation pulse is on. This scheme hence allowed the demonstration of high indistinguishability and high efficiency single photon emission for QDs in microcavities [24].

In the present work, we experimentally demonstrate that acoustic phonon-assisted excitation allows to fully exploit the polarization-selective optical selection rules of QDs charged by a single carrier (electron or hole). We demonstrate that this excitation scheme is compatible with subsequent monitoring of the dynamics and coherence of a single hole spin. We first observe the precession of a hole spin in a low transverse magnetic field through polarization and time resolved photoluminescence of a

negatively charged QD under pulsed excitation. These measurements also allow to extract a lower bound to the spin coherence time limited by the emission lifetime of the excited state. To access longer spin coherence times, we perform polarization-resolved 2-photon correlation measurements of a positively charged QD under continuous wave phonon-assisted excitation. Our measurements demonstrate a hole spin coherence time exceeding the radiative lifetime by more than one order of magnitude, an important step towards the implementation of the original Lindner and Rudolph scheme.

We study annealed InGaAs quantum dots emitting around $\lambda=927$ nm, embedded in a planar GaAs 2λ -cavity, surrounded by 16 pairs of AlAs/GaAs distributed Bragg reflector (DBR) on top and 34 at the bottom. The cavity region starts with a $\frac{\lambda}{2}$ GaAs layer below the quantum dots, with a n-type doping at 10^{18} cm $^{-3}$ stopping 25 nm before the QD layer. Above the QD layer, a 8-nm GaAs capping layer is followed by an undoped Al $_{0.33}$ Ga $_{0.7}$ As superlattice [17], with a total optical thickness of $\frac{3\lambda}{2}$. In the Bragg mirrors, the n-type (bottom) and p-type doping (top) are gradually increased further from the cavity to ensure good ohmic contacts: a voltage bias then allows a control of the charge of the quantum dot ground state.

The LA phonon-assisted excitation scheme is sketched in Fig.1 a. The pulsed excitation laser is blue detuned from the optical transition of the QD by roughly $\Delta\lambda = 1$ nm. During the excitation pulse (here ≈ 20 ps), the laser adiabatically dresses and undresses the QD ground and excited states while a fast relaxation of a longitudinal acoustical phonon allows for an efficient excited state population [21]. Overall, this achieves an incoherent population inversion, leaving the QD in the excited state with a probability above 85% [24]. In the present work, we also implement a continuous-wave (c.w.) LA phonon-assisted excitation scheme, that, while not allowing for high occupation probability, enables the exploration of long delay spin dynamics. The single photon emission from the QD is spectrally filtered from the excitation laser using high transmission, narrow bandpass filters (0.8 nm bandwidth) with no need for polarization filtering. The QD emission is then analyzed in polarization with waveplates and a polarizing beam-splitter, and detected with fast superconducting nanowire single photon detectors (time jitter ≈ 32 ps).

We first study the properties of the hole spin in the excited state of a negatively charged QD. The ground state consists of two degenerate electron spin states in the absence of magnetic field. In the excited state, an electron-heavy-hole pair is optically created in addition to the resident electron (X^- trion state). The two electron spins form a spin singlet, and the magnetic properties of the trion are determined by those of the unpaired hole only. Due to orbital angular momentum conservation, ground and excited states spin projections along the growth axis of the quantum dots ($\pm 1/2$ for the electron, $\pm 3/2$ for the

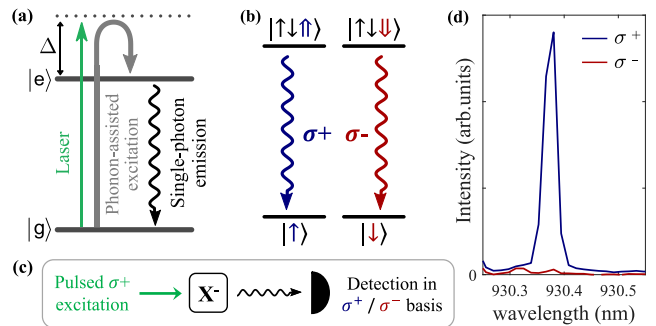


Fig. 1: (a) Schematic of the principle of LA excitation where a 20 ps laser pulse is detuned by $\Delta\lambda = 1$ nm from the trion transition. Acoustic phonon-assisted relaxation takes place between the laser-dressed QD states. Adiabatic undressing of the laser leaves the quantum dot in an excited state with high probability. (b) Energy levels and optical selection rules of the negatively charged QD in absence of magnetic field, with spin projections along the QD growth axis. (c) Schematic of the photoluminescence experiment. The negatively charged quantum dot is excited with σ^+ polarized laser pulses. The single photon emission is detected in the circular polarization basis using waveplates and polarizers. (d) Time-integrated spectrum of a negative trion under pulsed, circularly polarized acoustic phonon assisted-excitation.

heavy hole) result in polarization selective optical transitions involving circularly polarized photons (σ^\pm). The excitation is circularly polarized σ^+ pulsed laser light and the power is chosen to maximize the QD single-photon emission. Following the optical selection rules, the circularly polarized excitation populates only the trion excited state $|\uparrow\downarrow\uparrow\rangle$ (Fig. 1b). The single-photon emission is measured either along a parallel σ^+ or orthogonal σ^- circular polarization (Fig. 1c). If the hole remains in the same excited state during the whole spontaneous emission process, the single-photon is emitted with a polarization parallel to that of the laser. Emission in the orthogonal polarization can only occur if the QD undergoes a spin flip in the excited state within the spontaneous radiative decay lifetime. The time-integrated spectra in figure 1.d show hardly any emission in the polarization orthogonal to the excitation so that the corresponding time and spectrally-integrated intensities I_{σ^-} and I_{σ^+} verify $I_{\sigma^-} \ll I_{\sigma^+}$. This corresponds to a time-integrated degree of circular polarization, $D_{CP} = \left(\frac{I_{\sigma^+} - I_{\sigma^-}}{I_{\sigma^+} + I_{\sigma^-}} \right)$, of $94.7 \pm 0.2\%$ and demonstrates the excellent preservation of the polarization selection rules when using phonon-assisted excitation processes in contrast to other incoherent excitation schemes such p-shell excitation. This is consistent with previous observations for neutral excitons in both GaAs [25] and InGaAs QDs [24].

The same excitation scheme allows for monitoring the coherent Larmor precession of the hole spin in the excited state around an applied in-plane magnetic field (Voigt configuration). The magnetic field lifts the degeneracy

of both ground and excited states resulting in an energy splitting $\Delta E_{e/h}$ given by $\Delta E_{e/h} = \hbar g_{e/h} \mu_B B$ where $g_{e/h}$ are the transverse electron or hole Landé factor, μ_B is the Bohr magneton and B is the magnetic field strength. In this context, the states in Fig. 1.b are no longer eigenstates of the system Hamiltonian. At time t_0 , the QD is excited using a short σ^+ -polarized pulse laser pulse (i.e. of bandwidth greater than $\Delta E_{e/h}/\hbar$), and is initialized in state $|\uparrow\downarrow\uparrow\rangle$ (depicted as $|\uparrow\rangle$ in Fig. 2.a. for simplicity). The hole undergoes Larmor precession due to the magnetic field, and periodically oscillates between states $|\uparrow\rangle$ and $|\downarrow\rangle$. At a later time $t_0 + \tau$, the QD decays and emits either a σ^+ or σ^- polarized photon, depending on the spin state after the precession time of τ .

Figure 2.b shows the signature of the Larmor precession through the temporal evolution of the emitted intensities $I_{\sigma^+}(t)$ and $I_{\sigma^-}(t)$ during trion decay, for increasing applied magnetic fields up to 450 mT. Periodic oscillations are observed as the hole spin in the trion state coherently precesses at the Larmor frequency $g_h \mu_B B$. The sum of the two intensities (black line) is also displayed in the top panel of Fig. 2.b, displaying a monoexponential decay associated with the trion lifetime. Figure 2.c. presents the time-resolved *D**C**P*, which demonstrates only a slight damping of the oscillations over time. This indicates that the spin maintains its coherence well beyond the timescale of the radiative decay process.

We fit the evolution in Fig 2c using a simple model, where the master equation is numerically solved considering that the LA-assisted excitation process results in the same trion state populations as for resonant excitation. We also assume that the detected intensity I_{σ^+} (resp. I_{σ^-}) is directly proportional to the population of the trion state $|\uparrow\downarrow\uparrow\rangle$ (resp. $|\downarrow\downarrow\downarrow\rangle$) at any given time and we neglect the hyperfine interaction on the hole spin in the trion state. These measurements give access to an effective hole spin coherence time T_2^* which is dominated by a pure dephasing term. In the master equation of the model T_2^* is then reduced to a homogenous pure dephasing time.

With these hypothesis, the master equation yields a good fit for all the spin evolutions in Fig. 2c. using a trion radiative decay time $T_1^{(\text{trion})} = 450 \pm 20$ ps, $T_2^* \geq 15 \pm 5$ ns, and $g_h = 0.38 \pm 0.01$. This measurement provides a lower bound for $T_2^{(\text{spin})}$, limited by the lifetime of the excited state. The relatively high value of the transverse hole spin Landé factor g_h , which is typical in strongly annealed quantum dots [26], also implies that a relatively weak magnetic field is sufficient to implement a large number of precession cycles during the spin coherence time, which is significantly longer than the trion lifetime. All conditions are thus met to implement the LR scheme for cluster state generation with a dozen of photons.

The polarisation-resolved lifetime measurements thus give direct access to the properties of a hole spin in the

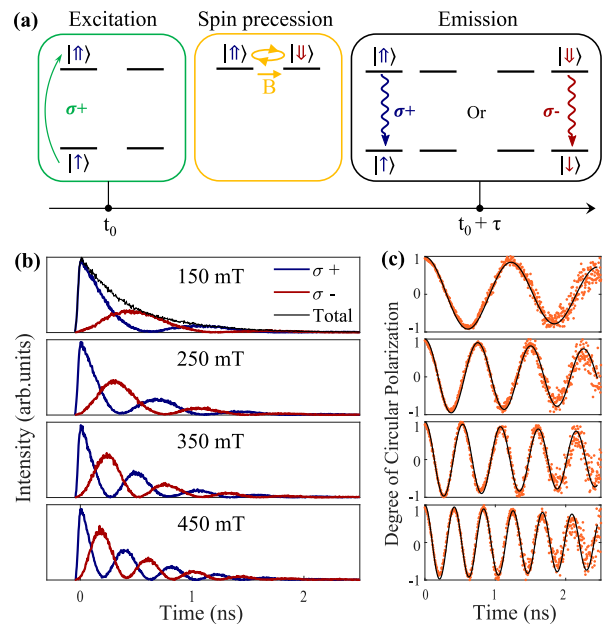


Fig. 2: (a) Schematic of the excited-state spin dynamics measurement. The negatively charged quantum dot is excited with σ^+ polarized laser pulses, populating only the state $|\uparrow\downarrow\uparrow\rangle = |\uparrow\rangle$. The in-plane magnetic field B induces a Larmor precession between the two trion spin states, and the emitted photons are detected in the circular parallel σ^+ or perpendicular σ^- polarization. (b) Polarization resolved time trace of the QD emission under in-plane magnetic field, and (c) corresponding degree of circular polarization *D**C**P*. The beatings reflect the coherent Larmor precession of the hole spin around the magnetic field. The lines are fit to the experimental data (see text).

excited state, but only provide a lower bound to the spin coherence time when it exceeds the trion lifetime by orders of magnitude. Moreover, the LR scheme would be more readily implemented with a hole spin in the ground state to generate many-photon linear cluster states owing to the reduced decoherence induced by nuclear spins [27]. To access the hole spin coherence time in the ground state, we propose and implement correlation measurements under continuous wave excitation.

We now consider a positively-charged QD with a hole in the ground state, and excite the positive trion transition again using the phonon-assisted excitation scheme. Figure 3.a. presents the optical selection rules corresponding to this situation, while Figure 3.b. details the experimental scheme used to probe the ground state hole spin dynamics. The excitation laser is now linearly polarized. In the absence of spin initialisation, the hole spin is in a mixed state with equal contributions from the $|\uparrow\rangle$ and $|\downarrow\rangle$ states, so that both trion transitions can be excited. The hole spin dynamics is then probed by recording the statistics of circularly cross-polarized emitted photons i.e. counting coincidence events between a σ^+ -polarized detected photon, and another σ^- -polarized

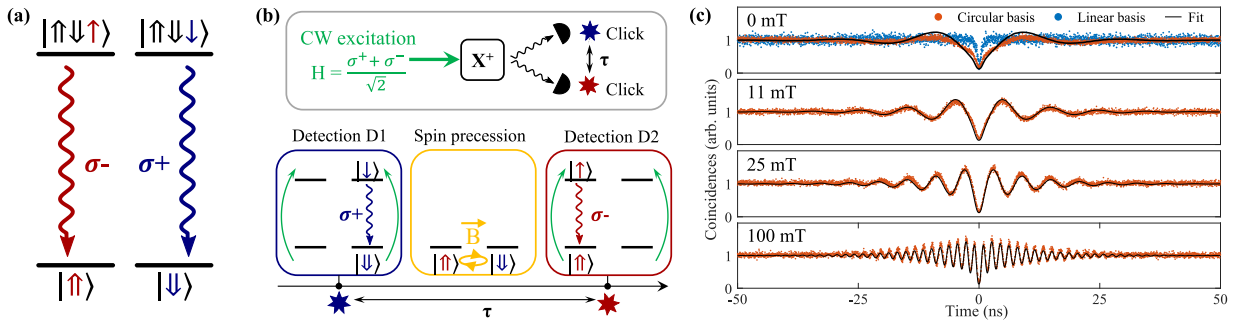


Fig. 3: (a) Energy levels and optical selection rules of the positively charged exciton with spin projections along the QD growth axis. (b) Schematic of the experiment. The positively charged quantum dot is LA-phonon assisted excited with linearly polarized, continuous laser light. The single photon emission is projected along two orthogonal bases with a set of waveplates and a polarizing beamsplitter. Cross-correlations are measured between the two detectors. (c) Cross-correlation measurements between orthogonal polarizations in the circular basis (σ_+/σ_-) (orange), and a linear basis (blue). The lines are fit to the experimental data (see text).

one, separated by a delay τ . Indeed, when a first photon is detected at time t_0 in polarization σ^+ , this leads to a projective spin measurement in the $|\downarrow\rangle$ ground state. This is followed by a precession of the ground state hole spin around the applied transverse magnetic field. The subsequent detection of a second σ^- -polarized photon at time $t_0 + \tau$ will therefore reflect the Larmor oscillation of the hole spin in the QD ground state after its initialization. We can thus measure the precession of the hole spin in the ground state through polarization-resolved cross-correlations between the two detectors. Mapping those cross-correlations to the spin population relies on using a low enough excitation power to limit multiple re-excitations. We also note that exciting with linear polarization prevents a dynamic nuclear polarization - i.e. polarisation of a nuclear spin induced by electron-nuclei spin flip-flop processes in the excited state [27]. Finally, the X^+ trion spin precession in the applied field or random Overhauser field during the trion radiative lifetime, is now time-averaged, and therefore reduces the contrast of the measured oscillations.

Fig. 3.c. shows the measured oscillations for increasing magnetic fields. The cross-correlations are measured through the coincidences between σ^+ and σ^- detection events, normalized to unity at long delays. At very short delays, an anti-correlation is always observed due to the single-photon nature of the emitted field. This anti-bunching is visualized when using a linear polarisation detection basis to remove the signature of spin-dependent correlations (blue data in the top panel of Fig. 3.c.). In the circular polarisation basis, after 1–2 ns, we observe a decaying oscillation of the cross-correlation signal, which is a signature of the ongoing Larmor precession between the spin states $|\uparrow\rangle$ and $|\downarrow\rangle$. In this regime, the cross-correlation oscillates between above- / below-unity values, as the $|\uparrow\rangle$ state becomes more / less populated than its equilibrium value at long delays when the hole spin is fully depolarized. We observe remaining oscillations

even when no magnetic field was applied indicating a small residual magnetic field of around 7 mT.

For further analysis of the results of Figure 3.c., we compare the experimental data with numerical simulations using the the same general framework as before. To mimic the CW excitation, we consider random excitation events in the very low excitation regime with only one excitation event within the relevant delays in the experiment. We obtain very similar parameters for both the trion lifetime $T_1^{(\text{trion})} = 450 \pm 80$ ps and the hole Landé factor $g_h = 0.4 \pm 0.01$. Here we can measure the spin coherence time, which reaches $T_2^{(\text{spin})} = 20 \pm 5$ ns for this QD, confirming that hole spins under LA-assisted excitation are suitable candidates for multi-photon entanglement processes within the LR scheme.

Note that we also include the hyperfine interaction of the electron spin in the trion states that reduces the fidelity of the optical readout process of the hole spin. The contrast of the oscillations in Fig. 3.c. is well reproduced by introducing this interaction in the frozen central spin model [28] where the electron spin is subject to a randomly-oriented mean field nuclear spin with a standard deviation of $\sigma_{\text{hf}}^{(e)} = 0.8 \mu\text{eV}$ [27]. Note that this value represents an upper bound since the oscillation contrast is also limited by experimental imperfections such as an imperfect projection to the circular polarization basis.

In conclusion, we have shown that acoustic phonon-assisted excitation is an excellent tool to measure a single spin-dynamics in quantum dots opening the path toward the implementation of the Lindner-Rudolph scheme for polarization-encoded cluster state generation. The detuning of the excitation wavelength compared to the resonant excitation scheme allows to use a simple spectral filtering to remove the excitation laser and preserve with high fidelity the optical selection rules. The direct monitoring of the hole spin precession in a low transverse

magnetic field also evidenced a heavy-hole spin coherence time of 20 ns in our sample, a value that is typical for a hole spin in the absence of nuclear spin control [29]. Such coherence time is two orders of magnitude larger than the trion radiative lifetime of a QD inserted in an optical cavity [30]. We thus anticipate that phonon-assisted excitation scheme should allow the efficient generation of long chains of entangled indistinguishable photons in linear cluster states.

Acknowledgements. This work was partially supported by the the IAD-ANR support ASTRID program Projet ANR-18-ASTR-0024 LIGHT, the QuantERA ERA-NET Cofund in Quantum Technologies project HIPHOP, the European Union’s Horizon 2020 FET OPEN project QCLUSTER (Grant ID 862035), the European Union’s Horizon 2020 Research and Innovation Programme QUDOT-TECH under the Marie Skłodowska-Curie Grant Agreement No. 861097 and the French RENATECH network, a public grant overseen by the French National Research Agency (ANR) as part of the ”Investissements d’Avenir” programme (Labex NanoSaclay, reference: ANR-10-LABX-0035). N.C. acknowledges support from the Paris Ile-de-France Région in the framework of DIM SIRTEQ.

-
- [1] N. H. Lindner and T. Rudolph, “Proposal for Pulsed On-Demand Sources of Photonic Cluster State Strings,” *Physical Review Letters* **103**, 113602 (2009).
- [2] W. B. Gao, A. Imamoglu, H. Bernien, and R. Hanson, “Coherent manipulation, measurement and entanglement of individual solid-state spins using optical fields,” *Nature Photonics* **9**, 363–373 (2015).
- [3] A. Delteil, Z. Sun, W.-b. Gao, E. Togan, S. Faelt, and A. Imamoglu, “Generation of heralded entanglement between distant hole spins,” *Nature Phys* **12**, 218–223 (2016).
- [4] R. Stockill, M. J. Stanley, L. Huthmacher, E. Clarke, M. Hugues, A. J. Miller, C. Matthiesen, C. Le Gall, and M. Atatüre, “Phase-tuned entangled state generation between distant spin qubits,” *Phys. Rev. Lett.* **119**, 010503 (2017).
- [5] C. Bonato, F. Haupt, S. S. R. Oemrawsingh, J. Gudat, D. Ding, M. P. van Exter, and D. Bouwmeester, “Cnot and bell-state analysis in the weak-coupling cavity qed regime,” *Phys. Rev. Lett.* **104**, 160503 (2010).
- [6] I. Schwartz, D. Cogan, E. R. Schmidgall, Y. Don, L. Gantz, O. Kenneth, N. H. Lindner, and D. Gershoni, “Deterministic Generation of a Cluster State of Entangled Photons,” *Science* **354**, 434–437 (2016).
- [7] M. Zwerger, W. Dür, and H. J. Briegel, “Measurement-based quantum repeaters,” *Phys. Rev. A* **85**, 062326 (2012).
- [8] K. Azuma, K. Tamaki, and H.-K. Lo, “All-photonic quantum repeaters,” *Nature Communications* **6**, 6787 (2015).
- [9] R. Raussendorf, D. E. Browne, and H. J. Briegel, “Measurement-based quantum computation on cluster states,” *Phys. Rev. A* **68**, 022312 (2003), publisher: American Physical Society.
- [10] N. Somaschi, V. Giesz, L. De Santis, J. C. Loredano, M. P. Almeida, G. Hornecker, S. L. Portalupi, T. Grange, C. Antón, J. Demory, C. Gómez, I. Sagnes, N. D. Lanzillotti-Kimura, A. Lemaitre, A. Auffeves, A. G. White, L. Lanco, and P. Senellart, “Near-optimal single-photon sources in the solid state,” *Nature Photon* **10**, 340–345 (2016).
- [11] H. Wang, Z.-C. Duan, Y.-H. Li, S. Chen, J.-P. Li, Y.-M. He, M.-C. Chen, Y. He, X. Ding, C.-Z. Peng, C. Schneider, M. Kamp, S. Höfling, C.-Y. Lu, and J.-W. Pan, “Near-transform-limited single photons from an efficient solid-state quantum emitter,” *Phys. Rev. Lett.* **116**, 213601 (2016).
- [12] T. Rudolph, “Why i am optimistic about the silicon-photon route to quantum computing,” *APL Photonics* **2**, 030901 (2017), <https://doi.org/10.1063/1.4976737>.
- [13] D. Cogan, Z.-E. Su, O. Kenneth, and D. Gershoni, “A deterministic source of indistinguishable photons in a cluster state,” (2021), 10.48550/ARXIV.2110.05908.
- [14] A. Kiraz, M. Atatüre, and A. Imamoglu, “Quantum-dot single-photon sources: Prospects for applications in linear optics quantum-information processing,” *Phys. Rev. A* **69**, 032305 (2004).
- [15] Y.-M. He, Y. He, Y.-J. Wei, D. Wu, M. Atatüre, C. Schneider, S. Höfling, M. Kamp, C.-Y. Lu, and J.-W. Pan, “On-demand semiconductor single-photon source with near-unity indistinguishability,” *Nature Nanotechnology* **8**, 213–217 (2013).
- [16] P. Senellart, G. Solomon, and A. White, “High-performance semiconductor quantum-dot single-photon sources,” *Nature Nanotechnology* **12**, 1026–1039 (2017).
- [17] N. Tomm, A. Javadi, N. O. Antoniadis, D. Najer, M. C. Lobl, A. R. Korsch, R. Schott, S. R. Valentin, A. D. Wieck, A. Ludwig, and R. J. Warburton, “A bright and fast source of coherent single photons,” *Nature Nanotechnology* (2021), 10.1038/s41565-020-00831-x.
- [18] K. Tiurev, P. L. Mirambell, M. B. Lauritzen, M. H. Appel, A. Tiranov, P. Lodahl, and A. S. Sørensen, “Fidelity of time-bin-entangled multiphoton states from a quantum emitter,” *Phys. Rev. A* **104**, 052604 (2021).
- [19] K. Tiurev, M. H. Appel, P. L. Mirambell, M. B. Lauritzen, A. Tiranov, P. Lodahl, and A. S. Sørensen, “High-fidelity multiphoton-entangled cluster state with solid-state quantum emitters in photonic nanostructures,” *Phys. Rev. A* **105**, L030601 (2022).
- [20] J. P. Lee, B. Villa, A. J. Bennett, R. M. Stevenson, D. J. P. Ellis, I. Farrer, D. A. Ritchie, and A. J. Shields, “A quantum dot as a source of time-bin entangled multi-photon states,” *Quantum Science and Technology* **4**, 025011 (2019).
- [21] P.-L. Ardel, L. Hanschke, K. A. Fischer, K. Müller, A. Kleinkauf, M. Koller, A. Bechtold, T. Simmet, J. Wierzbowski, H. Riedl, G. Abstreiter, and J. J. Finley, “Dissipative preparation of the exciton and biexciton in self-assembled quantum dots on picosecond time scales,” *Phys. Rev. B* **90**, 241404 (2014).
- [22] M. Cosacchi, F. Ungar, M. Cygorek, A. Vagov, and V. M. Axt, “Emission-frequency separated high quality single-photon sources enabled by phonons,” *Phys. Rev. Lett.* **123**, 017403 (2019).
- [23] C. Gustin and S. Hughes, “Efficient pulse-excitation techniques for single photon sources from quantum dots in

- optical cavities,” *Advanced Quantum Technologies* **3**, 1900073 (2020).
- [24] S. Thomas, M. Billard, N. Coste, S. Wein, Priya, H. Ollivier, O. Krebs, L. Tazaïrt, A. Harouri, A. Lemaitre, I. Sagnes, C. Anton, L. Lanco, N. Somaschi, J. Loredó, and P. Senellart, “Bright Polarized Single-Photon Source Based on a Linear Dipole,” *Phys. Rev. Lett.* **126**, 233601 (2021).
- [25] M. Reindl, J. H. Weber, D. Huber, C. Schimpf, S. F. Covre da Silva, S. L. Portalupi, R. Trotta, P. Michler, and A. Rastelli, “Highly indistinguishable single photons from incoherently excited quantum dots,” *Phys. Rev. B* **100**, 155420 (2019).
- [26] A. V. Trifonov, I. A. Akimov, L. E. Golub, E. L. Ivchenko, I. A. Yugova, A. N. Kosarev, S. E. Scholz, C. Sgroi, A. Ludwig, A. D. Wieck, D. R. Yakovlev, and M. Bayer, “Strong enhancement of heavy-hole Landé factor q in InGaAs symmetric quantum dots revealed by coherent optical spectroscopy,” (2021), 10.48550/ARXIV.2103.13653.
- [27] B. Urbaszek, X. Marie, T. Amand, O. Krebs, P. Voisin, P. Maletinsky, A. Högele, and A. Imamoglu, “Nuclear spin physics in quantum dots: An optical investigation,” *Rev. Mod. Phys.* **85**, 79–133 (2013).
- [28] I. A. Merkulov, A. L. Efros, and M. Rosen, “Electron spin relaxation by nuclei in semiconductor quantum dots,” *Phys. Rev. B* **65**, 205309 (2002).
- [29] R. J. Warburton, “Single spins in self-assembled quantum dots,” *Nature Materials* **12**, 483–493 (2013).
- [30] H. Ollivier, I. Maillette de Buy Wenniger, S. Thomas, S. C. Wein, A. Harouri, G. Coppola, P. Hilaire, C. Millet, A. Lemaitre, I. Sagnes, O. Krebs, L. Lanco, J. C. Loredó, C. Antón, N. Somaschi, and P. Senellart, “Reproducibility of high-performance quantum dot single-photon sources,” *ACS Photonics* **7**, 1050–1059 (2020).